Comparison of Soot Production from Direct-Injected Single and Two Component n-Paraffins in a Compression Ignition Engine

Energy and Environment Division ※Kevin Sholes Yuichi GOTO Hajime ISHII
Hisakazu SUZUKI Matsuo ODAKA

1. Introduction

In this study, fuel composition was investigated as a parameter influencing mixing of direct injected fuel with chamber air. It has been proposed that during direct injection of a two-component mixture of liquid fuels, in the two-phase region of the fuel mixture the rapid boiling of the lower boiling point component helps disperse the remaining liquid and thus accelerate the evaporation and mixing processes in comparison with a single component fuel. Utilizing this phenomenon through mixtures of fuels with widely different boiling points has potential for reducing particulate emissions from compression ignition engines. In this research, the physical characteristics of injected two-component mixed fuels were compared with single component fuels by visualization using a bottom-view type research engine. In cylinder soot production and flame temperature were analyzed using the two-color method. And, in-cylinder results were related to exhaust particulate measurements using the same fuels.

This investigation focuses on the influence of boiling point in single and 2-component mixtures of normal paraffins. Comparison is sometimes made with diesel, but not emphasized. Although an ultimate goal of this research is the development of alternative fuels, the tested fuels were chosen based on potential for illucidating properties affecting evaporation, mixing and particulate formation rather than their potential for direct application as alternate fuels.

2. Experimental Fuel Properties

Except for JIS No.2 diesel included for comparison, the tested fuels consisted of a range of normal parrafins. As shown in Table 1, as the chain length of these straight-chain, saturated hydrocarbons increases, the density, viscosity, boiling point, and cetane number all increase, while the latent heat of vaporization decreases. Because the boiling point and cetane number both increase with increasing chain length, the in-cylinder effects of boiling point can not easily be separated from the effects of cetane number. In this study, by mixing two n-parrafin components with differing chain lengths the effect of boiling point range was examined while holding the cetane number within a limited range.

Table 1. Pure Fuel properties [1]

n-paraffins	C_5H_{12}	C_6H_{14}	C_7H_{16}	C_9H_{20}	$C_{11}H_{24}$	$C_{13}H_{28}$
common name	pentane	hexane	heptane	nonane	undecane	tridecane
density, g/ml @ 15°C	0.631	0.665	0.687	0.730	0.746	0.762
kinematic viscosity, mm^2/s @ 30°C	0.336	0.429	0.538	0.878	1.405	1.999
boiling point, °C @ 1 atm	36.1	68.8	98.4	151.1	195.9	235.4
latent heat of vaporization, kJ/kg @ 1 atm	358.2	333.4	318.5	290.6	269.7	252.9
FIA Cetane Index	19	24	38	60	83	91

In total, testing included JIS No.2 diesel, n-nonane (C_9H_{20}), and two 2-component mixtures: n-heptane plus n-undecane (C_7H_{16}:$C_{11}H_{24}$) and n-pentane plus n-tridecane (C_5H_{12}:$C_{13}H_{28}$). In addition, particulate emissions were measured, but no in-cylinder visualization was performed, for n-hexane plus n-heptane plus 1% ethylhexylnitrate (C_6H_{14}:C_7H_{16}+EHN). The three two-component fuels were mixed in 50/50 volume ratios which resulted in mole ratios of 0.679:0.321 for C_5H_{12}:$C_{13}H_{28}$, 0.529:0.471 for C_6H_{14}:C_7H_{16}, and 0.589:0.411 for C_7H_{16}:$C_{11}H_{24}$. Ethylhexylnitrate (EHN) was added to the C_6H_{14}:C_7H_{16} mixture to raise the cetane number to a level acceptable for comparison with the other fuels in this study. Aside from cetane

improvement, EHN was ignored when considering other fuel properties of this mixture.

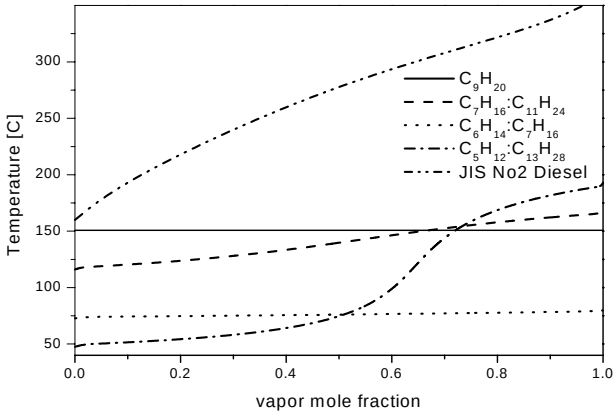

Figure 1. Distillation Curves

2. 1. Distillation Curves

The distillation curves for the five tested fuels are presented in Figure 1. Diesel evaporates at considerably higher temperatures than the other four fuels. The C_5H_{12}:$C_{13}H_{28}$ mixture has a step-like shape due to the the large difference in boiling points between n-pentane and n-tridecane. The low temperature evaporation is almost entirely from the n-petane component. In fact, at the 60% evaporation point only 1% of the vapor is n-tridecane. In terms of distillation the C_6H_{14}:C_7H_{16} mixture has a very small temperature range and thus approximates a pure fuel such as C_9H_{20}, also shown in Figure 1. This C_6H_{14}:C_7H_{16} mixture was particularly selected for this research because it has a 50% distillation point very similar to C_5H_{12}:$C_{13}H_{28}$.

2. 2. Two-Phase Region

While the distillation curves show the boiling ranges at atmospheric pressure, a different perspective is gained from the pressure-temperature phase diagram of Figure 2. In Figure 2, C_9H_{20} has a single vapor line terminating in the critical point. In contrast, the two-component mixtures have two-phase regions separating the liquid phase on the left from the gas phase on the right and no defined critical point. Within the two-phase region, shown shaded in Figure 2, liquid and vapor stages are in thermodynamic equilibrium with the proportions of each component in each phase varying smoothly according to changes in either temperature or pressure within the region. The wider the difference between the component boiling points, the broader is the two phase region. Moreover, the short-chain normal paraffins have their critical points at higher pressures so that the inclusion of a short chain normal paraffin tends to increase the height of the two-phase region to higher pressures.

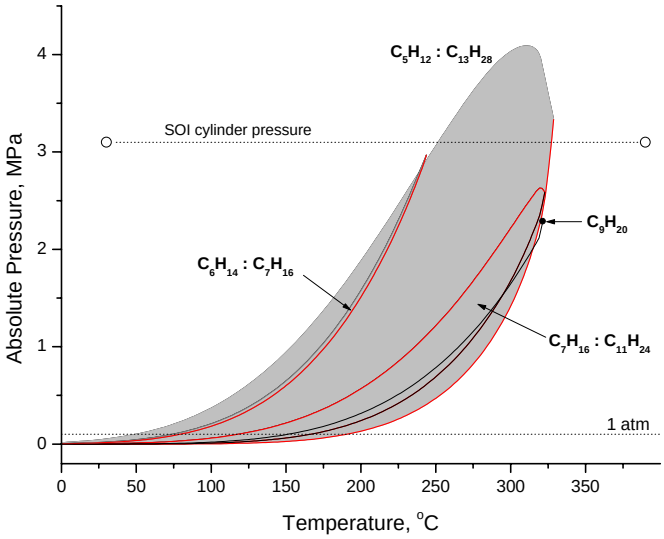

Figure 2. Two-Phase Region

The horizontal dashed line in Figure 2 indicates the cylinder pressure at start of injection for engine tests in this study. This curve shows that for injected fuel being heated and evaporated by the hot cylinder gas, the quasi-equilibrium pathway for these conditions would include passing through the two-phase region for the C_5H_{12}:$C_{13}H_{28}$ mixture. The cylinder pressure is higher than the highest point in the two-phase regions of the other two mixtures and higher than the critical point for C_9H_{20}. For these fuels the quasi-equilibrium pathway would consist of a smooth transition from compressed liquid to superheated gas with no definable boundary between the two states.

Senda et al. have advanced the hypothesis that under ambient conditions where injected fuel is heated and evaporates at a pressure such that the fuel passes through a two-phase region (C_5H_{12}:$C_{13}H_{28}$ in Figure 2), evaporation and mixing are enhanced by the phenomena of flash-boiling.[2] The basic premise is that the very fast vaporization of the low boiling point component causes a violent boiling that accelerates dispersion and evaporation of the higher boiling point component. In the fuel design concept by Senda et al., the flash boiling phenomena aids formation of a more uniformly disperse mixture, reduces locally fuel-rich regions, and leads to lower particulate emissions. The fuel choices in this study

allow a comparison between C_5H_{12}:$C_{13}H_{28}$ in which flash-boiling may be expected and three fuels in which flash-boiling is not possible.

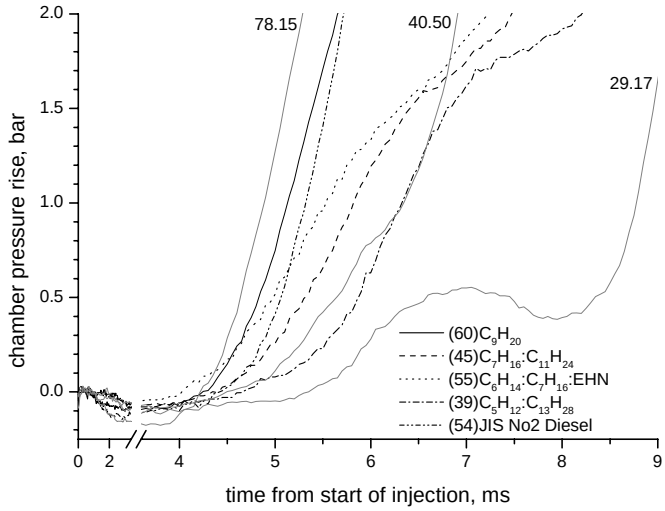

Figure 3. FIA-100 pressure traces

2．3．Cetane Number

Because it was impossible to completely eliminate the differences in cetane number in the choice of fuels, the differences in ignition delay were investigated with a fuel injection analyzer (FIA-100, Fueltech AS, Norway). In this device, air at high pressure is introduced into the 0.63 liter chamber and heated to a temperature of 723 K. When the chamber temperature and pressure are stabilized at the desired conditions, fuel is injected at 20 MPa into the quiescent chamber via a single-hole nozzle (0.35 mm hole diameter). The signal from a needle lift indicator mounted on the injector nozzle initiates recording of the chamber pressure. The duration from needle lift to the sudden pressure rise indicative of ignition indicates the ignition delay. These experiments are described in more detail in Sholes et al.[3]

FIA-100 reference curves for known cetane number fuels (provided by the manufacturer) were used to assign an FIA-100 cetane index to each fuel. The actual pressure curves representing the average of 20 injections for each fuel are shown in Figure 3 along with three sample reference fuels with known cetane numbers of 78.15, 40.50, and 29.17. This figure shows some of the details of initial combustion that is simplified by the assignment of a single cetane number. For instance, the addition of 1% ethylhexylnitrate to C_6H_{14}:C_7H_{16} causes an initial pressure rise at 4 ms that is more rapid than the 78.15 cetane number reference fuel, but because the slope is less steep the mixture quickly begins to resemble a much lower cetane number fuel. In determining an FIA-100 cetane index the pressure traces were compared to the reference fuel for the range of pressure rise including from 0.2 to 1.2 bar. The resulting cetane indices are indicated in parenthesis in the curve labels of Figure 3. The cetane indices range from 39 for C_5H_{12}:$C_{13}H_{28}$ to 60 for C_9H_{20}.

2．4．Summary of Fuel Properties

A summary of the above discussed fuel properties for the tested fuel mixtures is given in Table 2, which also includes density, viscosity, and lower heating value.

Table 2 Test Fuel Properties [1]

		C_5H_{12}:$C_{13}H_{28}$	C_7H_{16}:$C_{11}H_{24}$	C_9H_{20}	C_6H_{14}:C_7H_{16}	JIS No2 Diesel
Mole ratios		0.679:0.321	0.589:0.411	-	0.529:0.471	-
density, g/ml @ 15°C		0.708	0.719	0.730	0.675	0.828
kinematic viscosity, mm^2/s @ 30°C		0.713	0.844	0.878	0.480	3.461
distillation temperature, °C @ 1 atm	10%	51.9	120.9	151.1	80.8	198.0
	50%	75.1	140.2	151.1	83.3	284.0
	90%	182.1	162.6	151.1	85.8	332.5
LHV, kJ/g		44.473	44.348	44.312	44.642	43.2
FIA Cetane Index		39	45	60	55*	54

*with 1% added ethylhexylnitrate

Table 3 Engine Specifications and Test Conditions

Engine	Hino	AVL
Type	Single cylinder	Single cylinder
Cylinder head	4 valve	2 valve
Bore × Stroke, mm	135 × 150	85 × 94
Displacement	2.15 L	0.533 L
Compression ratio	16	17.4
Swirl ratio	2.2	2.0

Injection system	Common rail	In-line pump
Injection pressure	50 MPa	25 MPa
Speed	1000 RPM	1000 RPM
Equivalence ratio	0.45	0.45
Water Temperature	80°C	75°C

3. Experimental Equipment and Conditions

Engine experiments were divided between combustion analysis and emissions measurement using a Hino single-cylinder engine and visualization and two-color method experiments using an AVL single-cylinder, bottom-view type visualization engine. The specifications for the two engines are compared in Table 3. Although the compression and swirl ratios are similar, the engines have substantially different bores and injection pressures, which makes comparison of spray behaviour difficult. All experiments were conducted at 1000RPM at a medium load condition.

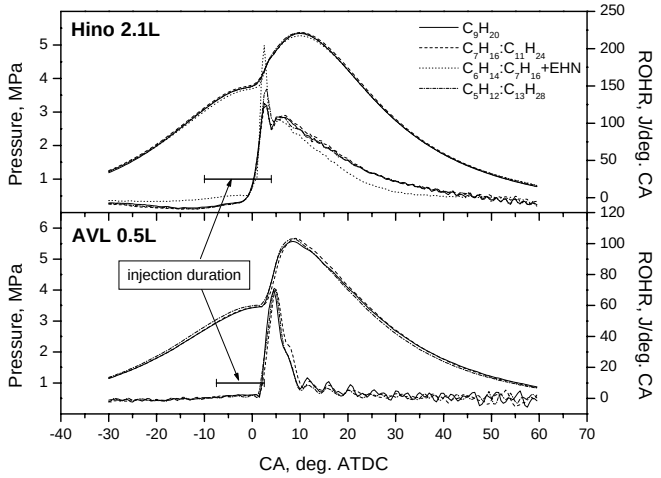

Figure 4. Pressure and Heat Release

4. Experimental Results

4. 1. Heat Release Analysis

Figure 4 shows pressure and heat release analysis for the two engines at the same equivalence ratio of 0.45. Results for diesel are not shown to emphasize the comparison between the normal paraffin fuels. Start of injection was -10° ATDC for the Hino engine and -7.5° ATDC for the AVL engine resulting in a start of ignition in the AVL engine delayed by 2°CA compared with the Hino engine. In general, the Hino engine displayed distinct premix and diffusion combustion regions while the smaller AVL engine did not show a distinguishable diffusion flame region.

The early heat releases are not clearly ranked by cetane index. Thus, although a range of FIA cetane index from 39 to 60 was measured, cetane index was considered to be only a small factor. The peak of the premix heat release rate for the Hino engine was very high for C_6H_{14}:C_7H_{16}+EHN, followed by C_5H_{12}:$C_{13}H_{28}$, with the remaining two about equal. The plausible explanation is that during the injection delay period a larger proportion of the fuels with the lower boiling point components evaporated and were available for combustion at the point of ignition. However, the high spike for C_6H_{14}:C_7H_{16}+EHN is also contributable to the cetane enhancer, and moreover, in the AVL engine the fuels showed equal peaks in the heat release rate. C_6H_{14}:C_7H_{16}+EHN was not tested in the AVL engine.

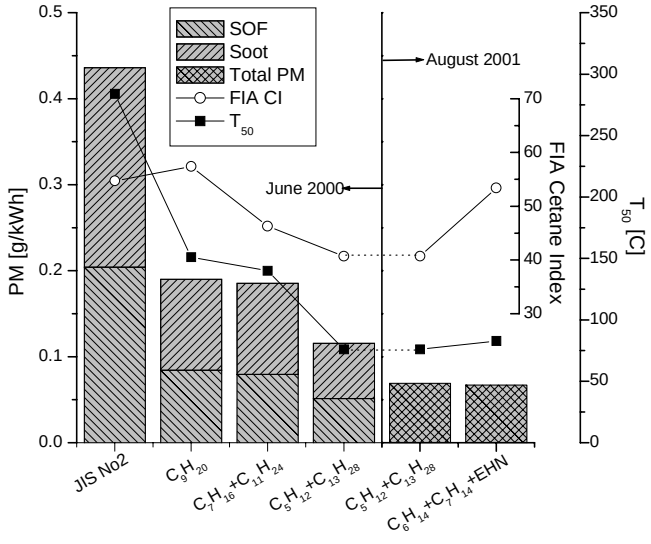

Figure 5. PM Measurements

4. 2. PM Measurements - Hino Engine

The purpose of experiments in the Hino engine was to compare emissions levels between the test fuels. These experiments are described in more detail in Suzuki et al.[4] In this discussion, only PM (particulate matter), which was measured gravimetrically in a full dilution tunnel, is considered.

Figure 5 compares the exhaust PM for the tested fuels. Measurements were made during two different periods separated by a year, and those measurements are separated left from right in the figure. The initial hypothesis of the benefits of two-component mixtures with large boiling point differences leading to flash-boiling during injection receives support in the data taken during June 2000. The C_5H_{12}:$C_{13}H_{28}$ mixture, the only mixture with the potential for flash-boiling, resulted in a 40% reduction in PM compared with C_7H_{16}:$C_{11}H_{24}$ and C_9H_{20}. However, in August 2001, C_5H_{12}:$C_{13}H_{28}$ was tested again along with C_6H_{14}:C_7H_{16}+EHN. Total PM was significantly lower than previously measured under the same conditions, leaving some doubt as to the repeatability of this data. Nevertheless, C_6H_{14}:C_7H_{16}+EHN resulted in exhaust PM as low as C_5H_{12}:$C_{13}H_{28}$ even though flash-boiling could not possibly play a factor with C_6H_{14}:C_7H_{16}+EHN.

Referring again to Figures 1 and 2, it is clear that the presence or absence of a two-phase region in the fuel phase diagram aside, the compared fuels have very different distillation characteristics. Therefore, T_{50} was arbitrarily chosen as a comparative measure of volatility and included in Figure 5. Without supplying any additional evidence for a causal relationship, it still may be said that T_{50} and exhaust PM correlate fairly well in this study. FIA cetane index is also included in the figure, which shows that the relationship between cetane index and PM is considerably less clear.

4. 3. Visualization - AVL Engine

4. 3. 1. AVL Engine Geometry

Coinciding with the Hino engine experiments, in-cylinder visualization of combustion with the tested fuels was performed in the AVL bottom-view engine. The purpose of these experiments was to investigate physical differences in spray and combustion behaviour that may explain measured differences in particulate emissions. The experiments included laser illuminated photography of the fuel injection phase and two-color method analysis of the combustion phase. All measurements were performed with an AVL 513D Engine Videoscope system and laser illumination for the fuel injection visualization was supplied by a 4 Watt argon ion laser.

4. 3. 2. Fuel Injection Visualization

Photography of the fuel spray led to the conclusion that the large scale identifying features of the fuel sprays of C_9H_{20}, C_7H_{16}:$C_{11}H_{24}$ and C_5H_{12}:$C_{13}H_{28}$ are not notably distinguishable. Though not measured, the spray angles appeared the same and no distinguishable differences in evaporation were observed. Notably, the appearance of a liquid core extending virtually to the wall of the bowl is troublesome for comparisons with the larger Hino engine where wall impingment is most likely not a factor.

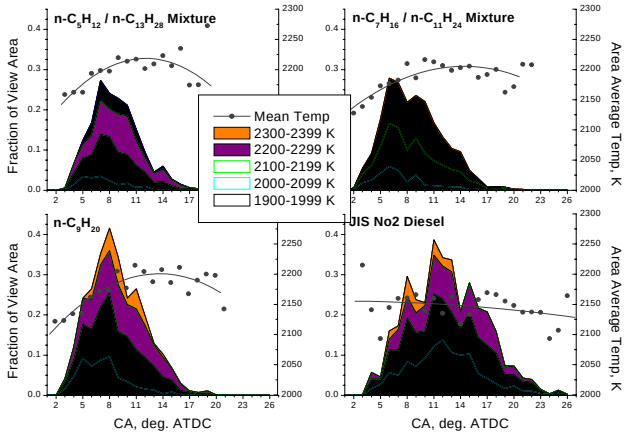

Figure 6. Flame Temperature Area Distribution

4. 3. 3. Flame Temperature

Next, combustion flame photography was performed for analysis using the two-color method. For statistical comparison, eight pictures were taken at each crank angle in increments of one degree crank angle from 1° ATDC to the end of visible flame. Figure 6 shows crank angle resolved flame temperature area distribution and mean flame temperature. In general, the mixtures with the most volatile fuel components had the smallest flame area overall. Also, C_5H_{12}:$C_{13}H_{28}$ had the shortest combustion duration while JIS No2 diesel had the longest. Similarly, the area average temperature was generally higher for the fuels with more volatile components. Thus, C_5H_{12}:$C_{13}H_{28}$ had the smallest flame area and highest average flame temperature, followed in order by C_7H_{16}:$C_{11}H_{24}$, C_9H_{20} and JIS No2 diesel. However, the area average temperature for the three normal paraffin fuels is very close at between 2170K and 2220K, while JIS No2 is lower at between 2120K and 2160K.

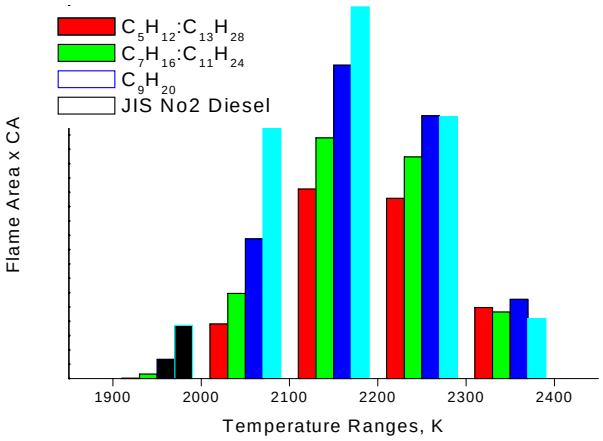

Figure 7. Integral of Flame Area Over Crank Angle

Flame area distribution by temperature was integrated over the entire combustion duration to yield Figure 7 which gives a breakdown of flame area by temperature. This figure makes clear that the differences in flame area are at the lower temperatures where the heavier fuels had far more integrated area. At the highest temperature region, 2300K-2400K, the integrated area is very similar for all four fuels.

Images of KL factor averaged over the 8 cycles of data were also compared to qualitatively visualize soot quantity throughout the combustion duration. In general, C_5H_{12}:$C_{13}H_{28}$ and C_7H_{16}:$C_{11}H_{24}$ showed very similar distributions with soot confined to the near wall area., while C_9H_{20} and JIS No2 had soot distributed over a considerably larger area.

5. Discussion

Fuel specifications may in part explain the two-color method results, which may in turn plausibly explain some of the features of the PM emission measurements. Fuels with high volatility components may be expected to evaporate and mix more quickly with cylinder air during the ignition delay period. Local rich regions would be reduced, reducing the area of visible flame, although the fuel-wall interaction must also be considered. The reduction of local rich regions reduces the areas burning at lower flame temperatures, which was a clear difference in the integrated flame area temperature distribution. These local rich regions are likely the source of the higher particulate emissions seen for C_9H_{20} and JIS No2 diesel.

6. Conclusions

The spray visualizations were not sufficient to either confirm or discredit any effects due to flash-boiling. For these effects to be analyzed it would be best to isolate them from engine effects and the optical constraints of performing these experiments in an engine. Future experiments could focus on light extinction or other drop sizing methods, shadowgraphy or schlieren in a heated bomb or rapid compression machine with fewer constraints on optical access. It is also likely that effects may only be visible at high camera magnification.

If the C_6H_{14}:C_7H_{16}+EHN results are not included, the PM data from the Hino engine lend support to the notion of a wide two-phase region in the fuels P-T diagram has benefits for fuel evaporation and fuel-air mixing which in turn reduces PM. However, it was shown that these results also correlate fairly well with T_{50}, the 50% point on the distillation curve. Although, the C_6H_{14}:C_7H_{16}+EHN results are insufficient and the experimental repeatibility requires further investigation to draw a stronger conclusion, the overall evidence suggests that low T_{50} is a better predicter of low PM emissions.

References

1. NIST Thermophysical Properties of Hydrocarbon Mixtures Database (Supertrapp), Version 3.0, U.S. Department of Commerce, National Institute of Standards and Technology, 1999.
2. Senda et al. "Fuel Design Concept Research for Low Exhaust Emissions by Use of Mixing Fuels," COMODIA 2001, The Fifth International Symposium on Diagnostics and Modeling of Combustion in Internal Combustion Engines, Nagoya, Japan, July 1-4, 2001.
3. Sholes et al., "Fundamental Study of Flash-Boiling Ignition by Fuel Ignition Analyzer," The 16th Internal Combustion Engine Symposium, Japan, September 5, 2000, pp. 73-78 (2000).
4. Suzuki et al., "Analysis of Emission Improvement Effects Using Two-Phase Region of Two-Component Mixed Fuel by Changing Injection Parameters," JSAE Fall Annual Meeting (2001). (in Japanese)